FtsH degrades dihydrofolate reductase by recognizing a partially folded species

Received: 6 June 2022 | Revised: 21 July 2022 | Accepted: 24 July 2022

DOI: 10.1002/pro.4410

FULL-LENGTH PAPER

THE PROTEIN SOCIETY WILEY

FtsH degrades dihydrofolate reductase by recognizing a partially folded species

Juhee P. Morehouse | **Tania A. Baker** | **Robert T. Sauer**

Department of Biology, Massachusetts Institute of Technology, Cambridge, Massachusetts, USA

Correspondence
Robert T. Sauer, Department of Biology, Massachusetts Institute of Technology, Cambridge, MA 02139, USA.
Email: bobsauer@mit.edu

Funding information
National Institutes of Health, Grant/Award Number: AI-16892

Review Editor: John Kuriyan

Abstract

AAA+ proteolytic machines play essential roles in maintaining and rebalancing the cellular proteome in response to stress, developmental cues, and environmental changes. Of the five AAA+ proteases in *Escherichia coli*, FtsH is unique in its attachment to the inner membrane and its function in degrading both membrane and cytosolic proteins. *E. coli* dihydrofolate reductase (DHFR) is a stable and biophysically well-characterized protein, which a previous study found resisted FtsH degradation despite the presence of an ssrA degron. By contrast, we find that FtsH degrades DHFR fused to a long peptide linker and ssrA tag. Surprisingly, we also find that FtsH degrades DHFR with shorter linkers and ssrA tag, and without any linker or tag. Thus, FtsH must be able to recognize a sequence element or elements within DHFR. We find that FtsH degradation of DHFR is noncanonical in the sense that it does not rely upon recognition of an unstructured polypeptide at or near the N-terminus or C-terminus of the substrate. Results using peptide-array experiments, mutant DHFR proteins, and fusion proteins suggest that FtsH recognizes an internal sequence in a species of DHFR that is partially unfolded. Overall, our findings provide insight into substrate recognition by FtsH and indicate that its degradation capacity is broader than previously reported.

KEYWORDS

AAA+ protease, degron, folding intermediate, membrane-bound protease, protein degradation, protein stability

1 | INTRODUCTION

Intracellular proteases enforce protein quality control and sculpt the cellular proteome in response to environmental stresses and changing nutritional landscapes. Within bacteria, most targeted proteolysis is carried out by proteases that belong to the AAA+ family (ATPases Associated with various cellular Activities).[1] These proteases contain ring-shaped AAA+ hexamers that use the energy of ATP hydrolysis to mechanically unfold specific protein substrates and then translocate the unfolded polypeptide through a central channel and into a degradation chamber for proteolysis. Initiation of degradation requires recognition of the substrate, usually by binding to a specific peptide sequence or tag, called a degron.[2] Degradation also requires the engagement of an

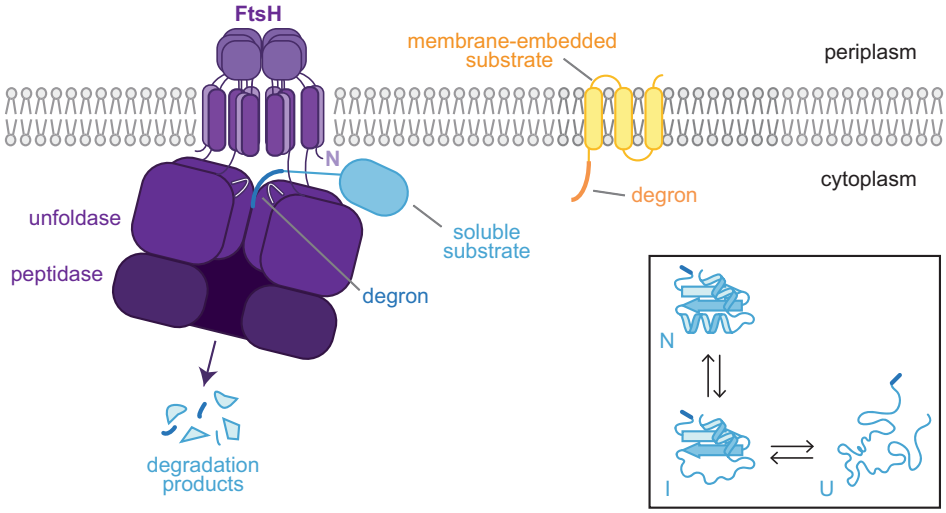

FIGURE 1 FtsH degrades membrane proteins and cytosolic proteins. *E. coli* FtsH is anchored to the inner membrane and degrades cytosolic proteins (blue) and membrane proteins (yellow) with appropriate degrons. Each FtsH subunit contains an N-terminal transmembrane helix, a periplasmic domain, another transmembrane helix, the cytoplasmic AAA+ unfoldase module, and a C-terminal metallopeptidase domain (colored from N- to C-terminus in light to dark purple). The cut-away view of the cytoplasmic portion of FtsH shows it pulling on the degron (dark blue) of a soluble substrate using conserved pore loops (white) to apply an unfolding force. After unfolding, the substrate is translocated through the axial channel and into the peptidase compartment for degradation. Inset. A cytoplasmic protein (light blue) with a terminal degron (dark blue) is shown in a folded or native state (N, top), a partially unfolded intermediate state (I, bottom left), and a globally unfolded state (U, bottom right)

unstructured segment of the substrate within the axial channel of the AAA+ ring.[3–5] This unstructured peptide can be the degron itself or located in another substrate region.

Escherichia coli encodes five AAA+ proteases: FtsH, ClpXP, ClpAP, Lon, and HslUV.[6] The membrane-bound FtsH protease is the only member of this enzyme family essential for *E. coli* growth.[7] Each subunit of the FtsH homohexamer consists of a transmembrane helix, a periplasmic domain, a second transmembrane helix, a AAA+ unfoldase module, and a zinc metallopeptidase domain (Figure 1).[8] The unfoldase and peptidase components, which constitute the proteolytic machinery of FtsH, reside on the cytoplasmic side of the inner membrane and play important roles in membrane-protein quality control and the degradation of some cytosolic proteins.[9,10] Different substrates are targeted for FtsH degradation by their C-terminal sequences, N-terminal sequences, or internal sequences.[9,11–16]

Based on biochemical studies of degron-tagged model proteins, *E. coli* FtsH (hereafter called FtsH) was found to degrade a variety of meta-stable proteins but not to degrade *E. coli* dihydrofolate reductase (hereafter called DHFR) or other stable substrates, unless the latter proteins were destabilized by mutation or circular permutation.[17] These results suggested that FtsH is a weak protein unfoldase, a property that could contribute to substrate selection *in vivo*. However, the idea that FtsH lacks robust unfoldase activity seems inconsistent with its ability to extract and degrade integral membrane proteins, which requires a substantial enzyme-generated force.[18,19] In thinking about this apparent paradox, we reasoned that the location of the FtsH axial channel, which faces the membrane, might require a sufficiently long segment of unfolded polypeptide between a protein and degron to allow recognition and engagement of substrates (Figure 1). By this model, FtsH would only degrade substrates that unfold completely or partially to generate an accessible degron (Figure 1, inset), or degrade stable substrates containing an extended unstructured tail and degron.

To test this model, we added tails composed of unstructured polypeptide linkers of different lengths and an ssrA degron to the C-terminus of DHFR and tested FtsH-dependent degradation. Indeed, a DHFR variant with a long linker and ssrA degron was degraded by FtsH. Unexpectedly, FtsH also degraded DHFR-ssrA variants with shorter linkers or no linker. Even more surprisingly, FtsH degraded DHFR with no appended degron. Our results indicate that FtsH recognizes an internal sequence in DHFR, which becomes accessible in a partially structured intermediate that equilibrates with native DHFR in degradation reactions. In contrast to most substrates of AAA+ proteases, DHFR sequences near either its N- or C-terminus appear to play little role in FtsH recognition. We discuss the implications of these

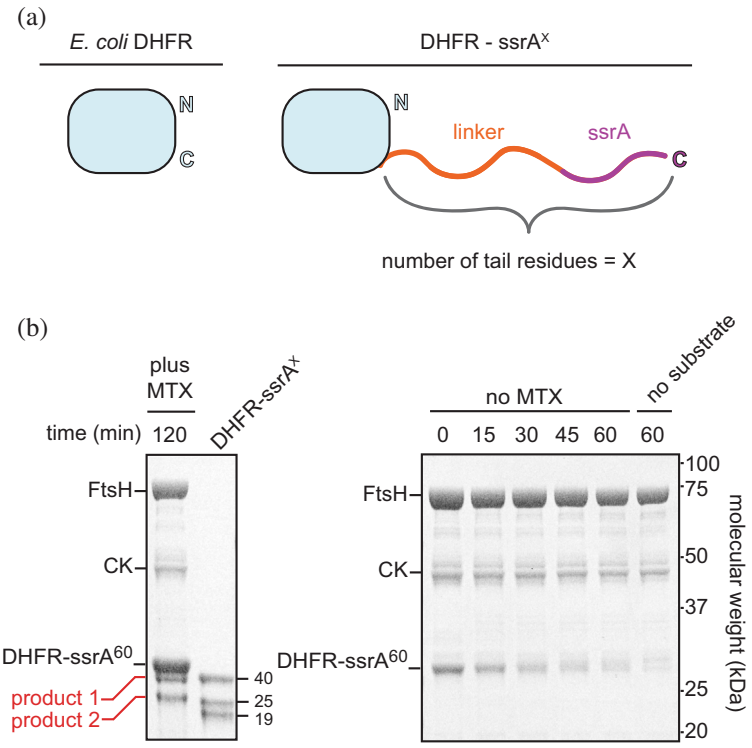

FIGURE 2 FtsH degrades DHFR-ssrA^{60}. (a) Cartoon depiction of DHFR with the N- and C-termini indicated (left) and of DHFR with a C-terminal tail consisting of linker (orange) and ssrA tag (purple; right). (b) SDS-PAGE of degradation assays. The left lane of the left panel shows DHFR-ssrA^{60} (20 μM) incubated for 120 min at 42°C with FtsH$_6$ (1 μM), ATP, a creatine kinase regeneration mix (CK), and MTX (100 μM). The right lane shows DHFR-ssrA^{40}, DHFR-ssrA^{25}, and DHFR^{19} as molecular weight standards (5 μM each). The right panel shows DHFR-ssrA^{60} (4 μM) incubated with FtsH$_6$ (1 μM), ATP, and a creatine-kinase based regeneration mix (CK), for different times at 42°C in the absence of MTX. The rightmost lane is a control without DHFR-ssrA^{60}. For both panels, the gel shown is representative of two independent experiments

findings in terms of the role of FtsH in the degradation of membrane and cytoplasmic proteins and in light of recent insights into FtsH structure from cryo-EM studies.

2 | RESULTS

We chose DHFR for several reasons. First, it is well characterized in terms of its structure, thermodynamic and kinetic stability, dynamics, and the effects of mutations on these properties.[20–22] Second, a prior study reported that DHFR with a C-terminal ssrA degron was not degraded by FtsH,[17] allowing us to test if extending the linker between DHFR and the ssrA tag might allow degradation. Third, the methotrexate (MTX) inhibitor stabilizes DHFR and prevents or dramatically slows degradation by AAA+ proteases.[21–24]

2.1 | FtsH degrades *E. coli* DHFR with a 60-residue degron tail

We constructed DHFR-ssrA^{60} with a 49-residue linker plus the 11-residue ssrA tag (60 total tail residues; Figure 2a), anticipating that FtsH would recognize and translocate the extended tail of this substrate until reaching the native DHFR domain. Then, we expected the release of a truncated degradation product consisting of undegraded DHFR with a portion of the 60-residue tail attached as an extension, as seen in similar experiments with other AAA+ proteases.[23] We observed this outcome in degradation reactions in the presence of MTX as assayed by SDS-PAGE (Figure 2b, left panel). Specifically, degradation of 20 μM DHFR-ssrA^{60} by 1 μM FtsH for 120 min resulted in the undegraded substrate and two product bands smaller than full-length DHFR-ssrA^{60}, consistent with proteolytic trimming of the ssrA^{60} tail. Comparison with DHFR variants containing tails of different lengths suggested that the undegraded extensions in the partial degradation products were ~28 and ~39 residues long, respectively. The ~28-residue extension is likely to have been within the FtsH channel or protease chamber when degradation stopped, suggesting that the native portion of MTX-bound DHFR in the product was pulled against the FtsH channel opening. We then assayed the kinetics of degradation of DHFR-ssrA^{60} by FtsH in the absence of MTX (Figure 2b, right panel). Surprisingly, FtsH degraded the entire DHFR-ssrA^{60} protein as judged by the absence of partial degradation fragments at the 60-min time point, when little of the original substrate remained.

2.2 | FtsH degrades untagged DHFR similarly to degron-tagged DHFR variants

We anticipated that FtsH would fail to degrade DHFR when the ssrA-tail became too short to allow

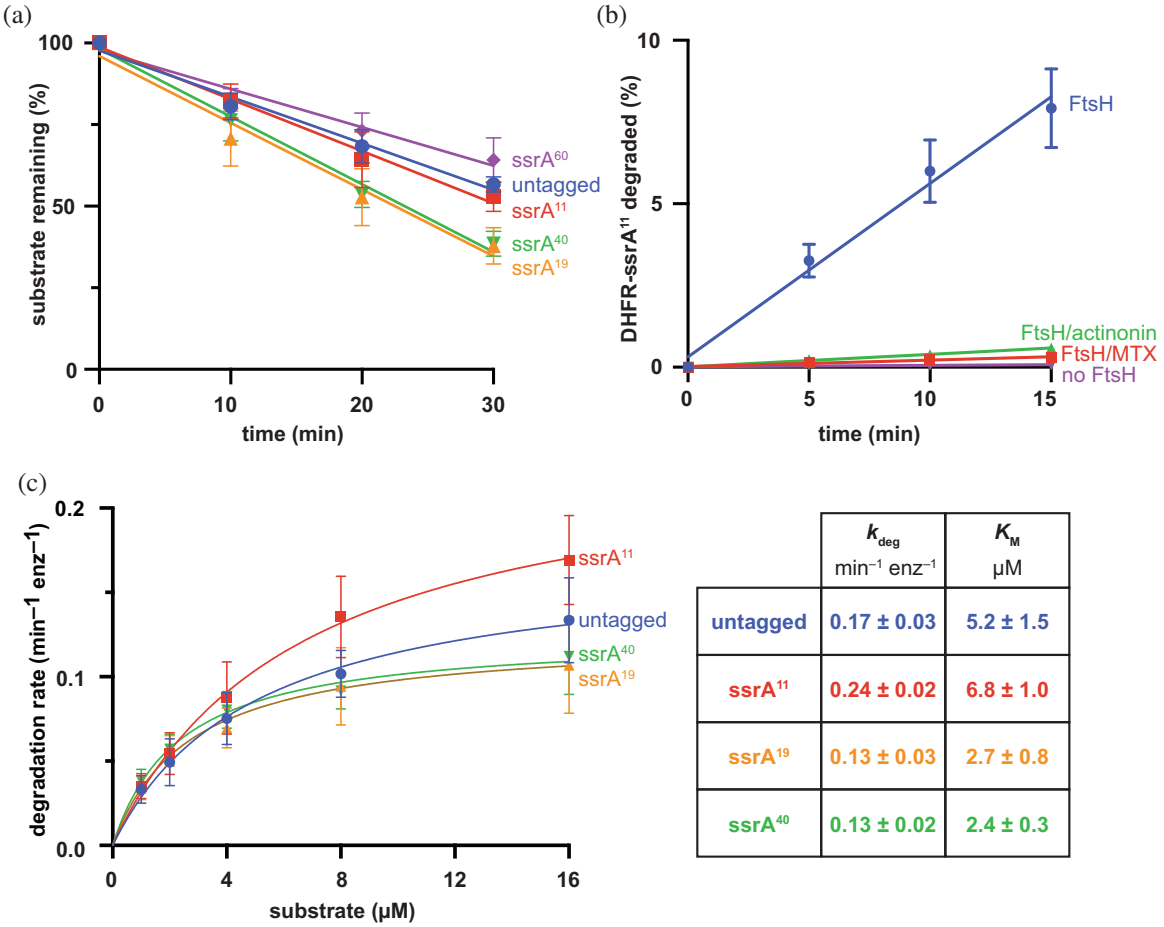

	k_{deg} min^{-1} enz^{-1}	K_M μM
untagged	0.17 ± 0.03	5.2 ± 1.5
ssrA^{11}	0.24 ± 0.02	6.8 ± 1.0
ssrA^{19}	0.13 ± 0.03	2.7 ± 0.8
ssrA^{40}	0.13 ± 0.02	2.4 ± 0.3

FIGURE 3 FtsH degradation of DHFR constructs. (a) Rates of $FtsH_6$ (1 μM) degradation of untagged DHFR or different DHFR-ssrA tail variants (5 μM each) at 42°C. Values are means ($n \geq 3$) ± 1 SD, and lines are linear least square fits. (b) Fluorophore-labeled DHFR-ssrA^{11} (16 μM) was incubated with $FtsH_6$ (0.5 μM), ATP, and a creatine-kinase regeneration mix at 37°C, and degradation kinetics were monitored by measuring the fluorescence of acid-soluble peptides released. Experiments are also shown in the presence of the actinonin inhibitor (10 μM), methotrexate (125 μM), or the absence of FtsH. (c) (Left) Rates of $FtsH_6$ degradation of different concentrations of untagged DHFR or DHFR-ssrA tail variants at 37°C. Values are means ($n \geq 3$) ± 1 SD. Lines are nonlinear least squares fit to the Michaelis–Menten equation. (Right) Average k_{deg} and K_M values ±1 SD from three or four independent experiments

engagement. However, FtsH degraded variants with tails of 40, 19, and 11 residues and even degraded untagged DHFR (Figure 3a). Although untagged DHFR was included as an intended negative control in this experiment, we were surprised to find that it was degraded at a rate generally similar to the degron-tagged variants in the SDS-PAGE degradation experiments.

Next, we tested the possibility that FtsH might degrade the ssrA-tailed and untagged DHFR substrates with substantially different steady-state kinetic parameters. For these experiments, we labeled the only solvent-exposed cysteine residue of DHFR, Cys^{152}, with a maleimide-fluorophore and used time-dependent increase in acid-soluble fluorescent peptides as an assay for the rate of FtsH degradation of DHFR-ssrA^{40}, DHFR-ssrA^{19}, DHFR-ssrA^{11}, and untagged DHFR. Figure 3b shows the linear time-dependent increase in acid-soluble fluorescent peptides reflecting FtsH degradation of 16 μM DHFR-ssrA^{11}. This degradation was prevented or greatly slowed (Figure 3b) when FtsH was omitted from the assay, when MTX was added to stabilize DHFR, or in the presence of actinonin, a small molecule that inhibits the peptidase activity of FtsH.[25]

We determined K_M and k_{deg} for degradation of untagged DHFR or different ssrA-tagged DHFR variants by measuring degradation rates as a function of substrate concentration and fitting the results to the Michaelis–Menten equation (Figure 3c, left panel). Although these values varied within an ~2-fold range when comparing different substrates, the only trend was that the two shortest proteins, untagged DHFR and DHFR-ssrA^{11}, were degraded somewhat faster at saturating substrate concentrations. Overall, however, FtsH degraded untagged DHFR, DHFR-ssrA^{11}, DHFR-ssrA^{19}, and

DHFR-ssrA[40] with similar degradation parameters (Figure 3c, right panel), indicating that the addition of an accessible ssrA-tail does not markedly increase the degradation rate of untagged DHFR.

2.3 | ATP cost of degradation

Substrates typically alter the rate of ATP hydrolysis by AAA+ proteases.[26] Indeed, near-saturating concentrations of untagged DHFR, DHFR-ssrA[11], DHFR-ssrA[19], or DHFR-ssrA[40] increased the rate of ATP hydrolysis by FtsH by 10–20% (Figure 4). Although this small increase may not be mechanistically important, these results support our model that untagged DHFR and the ssrA-tagged variants are being engaged, unfolded, and degraded by FtsH. By dividing the ATP-hydrolysis rates by the corresponding k_{deg} values for each protein (0.13–0.24 min^{-1}), we calculated that 430–890 ATPs are hydrolyzed by FtsH in the time required to bind, unfold, translocate, and degrade one molecule of each DHFR substrate. For comparison, FtsH degradation of the degron-tagged GlpG membrane protein uses 380–550 ATPs ($k_{deg} \approx 0.25$ min^{-1}; Reference 18) and ClpXP degradation of the titin^{I27}-ssrA substrate uses ~640 ATPs ($k_{deg} \approx 0.18$ min^{-1}; Reference 26). Hence, the energetic cost of DHFR degradation by FtsH is on par with degradation of other substrates that are degraded at comparably slow rates by FtsH or ClpXP.

2.4 | Which molecular DHFR species does FtsH recognize and degrade?

Most substrates of AAA+ proteases have unstructured degrons at or near a terminus, which provide both a specific recognition region and an unstructured peptide segment where the protease initiates the translocation/unfolding cycles required for degradation.[1,6] However, the N- and C-terminal residues of native DHFR make interactions that are part of its three-dimensional fold.[22,27] Thus, the termini of native DHFR are unlikely to function as FtsH recognition and/or initiation elements. Moreover, we show later that the M20 loop of DHFR is not required for FtsH degradation, even though this loop contains the only unstructured residues in the crystal structure of DHFR without bound ligands.[22] Hence, native DHFR is unlikely to be recognized and engaged by FtsH.

If FtsH only degrades the small population of DHFR molecules that is globally unfolded under equilibrium conditions, then a mutation that increases the thermodynamic stability of native DHFR relative to globally

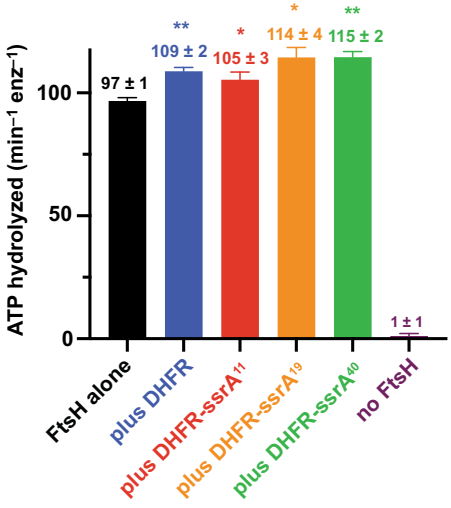

FIGURE 4 ATP hydrolysis. Rates of ATP hydrolysis at 37°C by $FtsH_6$ (0.5 μM) were measured in the absence of substrate or presence of untagged or ssrA-tagged DHFR proteins (20 μM each). A control reaction with no FtsH is included to show the background. Values are means ($n = 3$) ± 1 SD. Statistics (*$p < .05$ and **$p < .005$) were calculated by unpaired *t*-tests with Welch's correction (Welch's *t*-test), comparing each "plus substrate" group to the "FtsH alone" group

unfolded DHFR should decrease the degradation rate. This model predicts that the A145T mutation, which increases DHFR stability by ~3 kcal/mol,[28] would decrease the equilibrium fraction of unfolded DHFR by a factor of ~100-fold and thus slow FtsH degradation dramatically. By contrast, as shown in Figure 5a, FtsH degraded ^{A145T}DHFR slightly faster than untagged wild-type DHFR (^{WT}DHFR). We interpret this result as evidence that globally unfolded DHFR is not the primary FtsH degradation target.

Next, we tested FtsH degradation of two destabilized mutants, ^{W133V}DHFR and ^{I155A}DHFR, which are ~4 kcal/mol less stable than ^{WT}DHFR,[29,30] FtsH degraded these variants ~3-fold faster than ^{WT}DHFR (Figure 5b). However, these degradation rates would be expected to be substantially faster if FtsH exclusively recognized and degraded globally denatured DHFR. Hence, the rates of FtsH degradation of both stabilized and destabilized variants are inconsistent with a model in which globally unfolded DHFR is the major recognition target. Nevertheless, the W133V and I155A mutations appear to increase the equilibrium population of a molecular species that FtsH does recognize and degrade. Structural intermediates between fully denatured and native DHFR have been identified in folding/unfolding experiments and would be expected to represent a fraction of the equilibrium population at the 37–42°C temperatures of our degradation experiments.[31–33] Unfolded regions in these

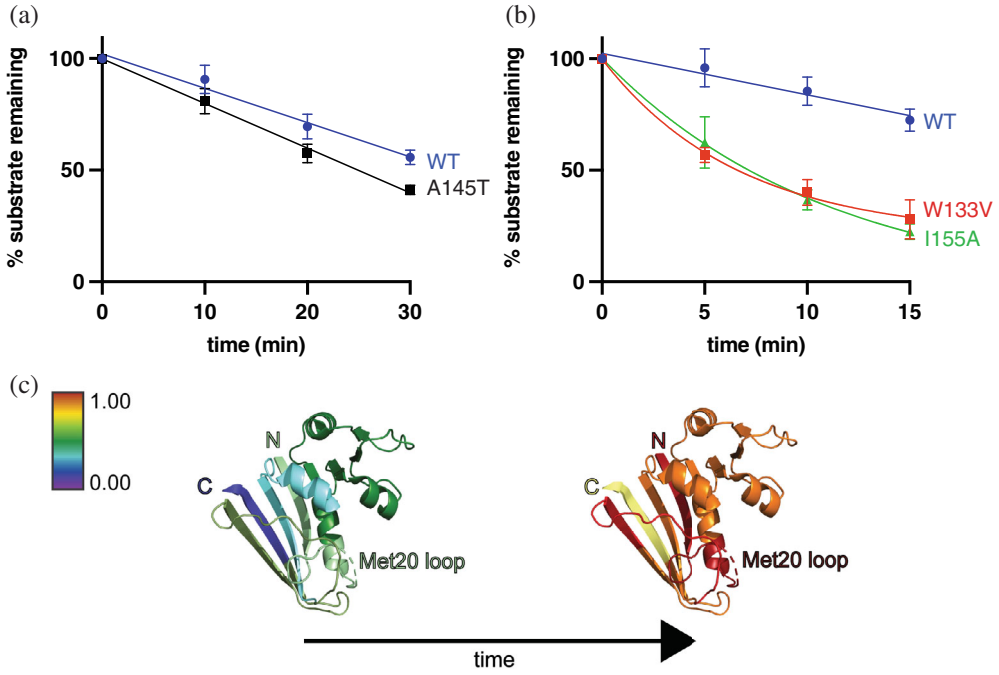

FIGURE 5 Effect of DHFR mutations on FtsH degradation. (c) ^{WT}DHFR or ^{A145T}DHFR (5 μM each) were incubated with $FtsH_6$ (1 μM), ATP, and a creatine-kinase regeneration mix at different times at 42°C, prior to assessing degradation by SDS-PAGE. The lines are linear least square fits. Data points are means ($n \geq 3$) ± 1 SD. (b) FtsH degradation of ^{WT}DHFR, ^{W133V}DHFR, and ^{I155A}DHFR using panel (a) conditions. A linear least-squares fit is shown for ^{WT}DHFR and single-exponential fits are shown for ^{W133V}DHFR and ^{I155A}DHFR. (c) Fluctuation map of DHFR (PDB code 5DFR) with colors of different segments based on the fraction of deuterium incorporation from 0.00 (purple) to 1.00 (dark red) at the beginning (left) and end (right) of an H/D exchange experiment[34]

intermediates are likely to correspond to those that exchange rapidly in H/D studies (Figure 5c).[34] It seems likely, therefore, that one or more of these partially folded protein species is recognized and degraded by FtsH.

2.5 | Sequence determinants of DHFR recognition

To investigate potential FtsH binding sites in DHFR, we used ^{35}S-FtsH to probe a peptide microarray consisting of 15-residue DHFR peptides offset from each other by two amino acids (Figure 6a). FtsH bound a group of overlapping peptides from three internal regions of DHFR: residues 19–47 (region 1); residues 43–67 (region 2); and residues 93–117 (region 3) (Figure 6a–c).

The DHFR peptides bound by FtsH surround the MTX-binding site in the three-dimensional structure (Figure 6c) and also overlap sequences with high B-factors in the crystal structure of unliganded DHFR.[22,27] The peptide-binding regions also include α-helical regions of DHFR and regions that experience the highest degree of H/D exchange (Figure 5c). Notably, FtsH did not bind to either N- or C-terminal peptides of DHFR in the peptide array.

The side chains of Leu[28] and Ala[29] are exposed on the surface of α-helix 1 in DHFR and are present in the first five peptide spots of region 1 (Figure 6a–c). When we mutated both residues to aspartic acids (L28D/A29D), the rate of FtsH degradation was reduced 2- to 3-fold compared to ^{WT}DHFR (Figure 6d), suggesting that the wild-type side chains at these positions contribute to recognition. However, the modest decrease in degradation also indicates that the full recognition element is more complex. We probed the effects of additional mutations throughout DHFR in an attempt to find alterations that slowed FtsH degradation by weakening binding. For example, we introduced the N23D/L24D, K32A/R33A/K38A, R33A, R33D, or R52D mutations, but FtsH degraded each mutant at a rate similar to ^{WT}DHFR. We did find that FtsH degraded variants with the A6D/A7D, R52A, K58A, K58D, R52A/R57A/K58A, G67T, or K106A/K109A mutations 2- to 3-fold faster than ^{WT}DHFR. Enhanced degradation of these variants probably results from an increase in the equilibrium population of a partially folded species that are recognized and degraded by FtsH.

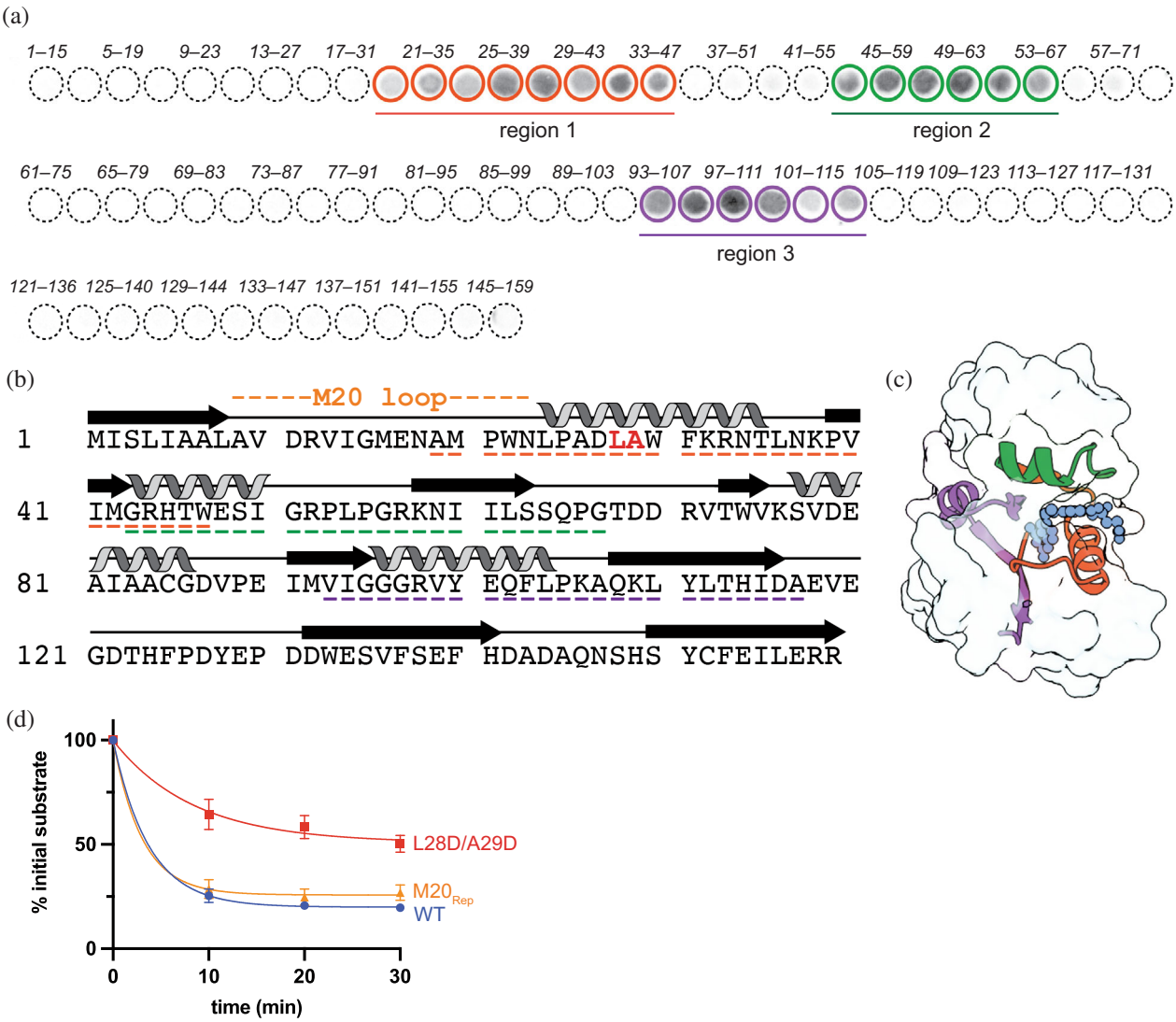

FIGURE 6 DHFR peptides that bind FtsH. (a) ^{35}S-FtsH binding to an array of DHFR peptides detected by autoradiography. Each circle represents a 15-residue DHFR peptide (every other spot labeled in italics), with the rightward neighboring spot shifted toward the C-terminus by two amino acids. Circles with solid lines mark peptides that bound ^{35}S-FtsH. (b) DHFR sequence and secondary structure. The M20 loop is labeled and Leu^{28} and Ala^{29} are colored red. Underlined residues are present in one or more FtsH-binding peptides from panel (a). (c) DHFR (PDB code 1RG7) is shown as an outlined transparent surface with methotrexate (blue) shown in ball-and-stick representation. Secondary structural elements in regions 1 (orange), 2 (green), and 3 (purple) are shown in the cartoon representation. (d) $FtsH_6$ (3 μM) degradation of ^{WT}DHFR, ^{M20rep}DHFR, and $^{L28D/A29D}$DHFR (5 μM each) at 42°C in the presence of ATP and a creatine-kinase (CK) regeneration mix was monitored by SDS-PAGE. Values are means ($n = 3$) ± 1 SD; lines are single-exponential fits

The M20 loop is highly dynamic in H/D exchange experiments (Figure 5c), and residues 16–20 of this loop are the only amino acids without electron density in the crystal structure of DHFR without bound ligands.[22] To test if engagement/initiation of FtsH degradation requires this loop, we replaced the complete M20 sequence (residues 9–24) with a GGGGS linker. However, FtsH degraded the resulting variant (^{M20rep}DHFR) at a rate similar to ^{WT}DHFR (Figure 6d). Thus, the M20 loop is dispensable for FtsH degradation.

2.6 | Domain fusions provide insight into initiation of degradation

If the FtsH recognition element in DHFR is accessible in a partially unfolded species, then residues at either the N or C terminus of DHFR might still serve as sites where FtsH begins translocation and subsequent unfolding. To test this model, we fused a HaloTag domain (Halo) to both termini of DHFR to create Halo-DHFR-Halo (Figure 7a). We chose Halo because it is not degraded by

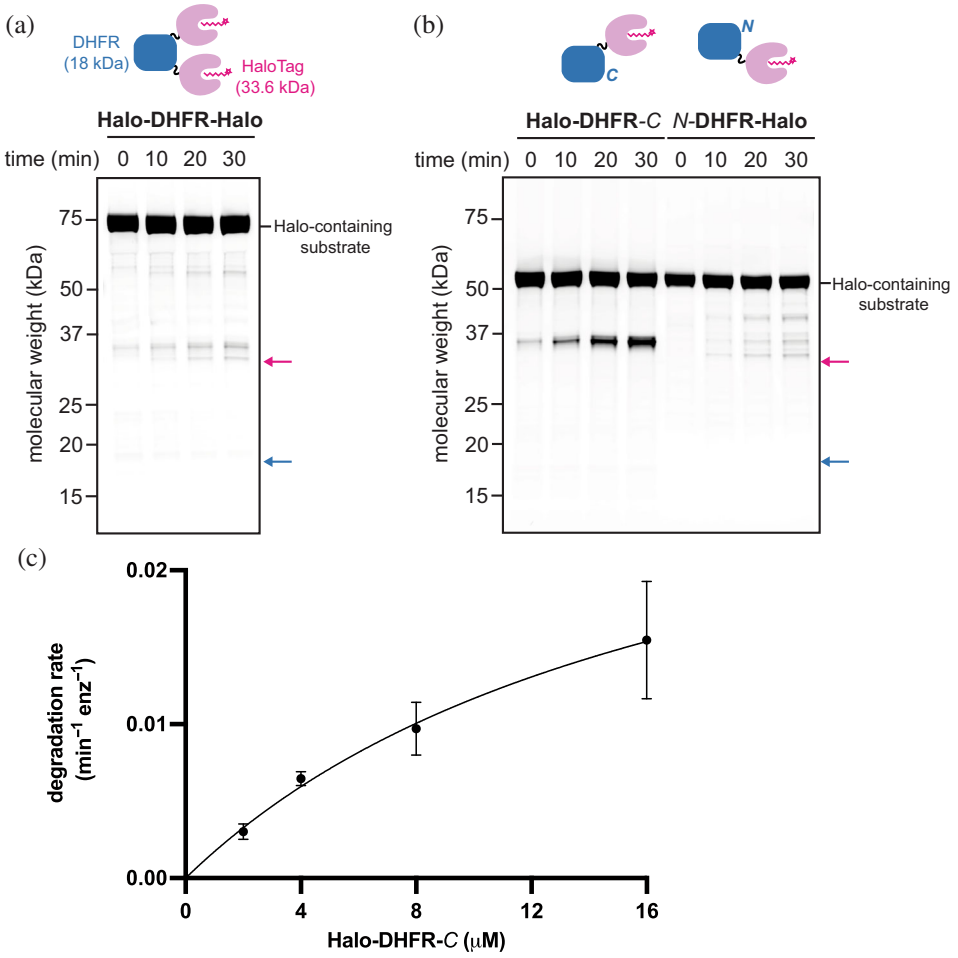

FIGURE 7 FtsH degradation of DHFR fused to fluorescent Halo domains. (a) Top, cartoon of fusion construct. Bottom, SDS-PAGE assay of the kinetics of degradation of Halo-DHRF-Halo (5 μM) by $FtsH_6$ (1 μM) at 42°C with ATP, and a CK regeneration mix. The pink and blue arrows show the expected mobilities of a free Halo domain and DHFR, respectively. (b) Top, cartoons of fusion constructs. Bottom, SDS-PAGE assay of the kinetics of degradation of Halo-DHFR-*C* or *N*-DHFR-Halo (5 μM) by $FtsH_6$ (1 μM). Conditions as in panel (a). (c) H (c) Rates of $FtsH_6$ (0.5 μM) degradation of different concentrations of Halo-DHFR-*C* at 37°C were determined by SDS-PAGE. The line is a non-linear least square fit of the data to the Michaelis–Menten equation; $k_{deg} = 0.03 \pm 0.02\ min^{-1}\ enz^{-1}$ and $K_M = 18 \pm 6.9$ μM. Values are means ($n \geq 3$) ± 1 SD

FtsH and can be covalently modified with tetramethylrhodamine (TMR), allowing visualization of any Halo-containing degradation products using fluorescence.[35,36] FtsH degraded Halo-DHFR-Halo, albeit slowly, generating fluorescent products (Figure 7a). This result indicates that access to residues at the N or C terminus of DHFR is not necessary for FtsH degradation and provides additional support for engagement of an internal sequence or sequences in DHFR for initiation of degradation.

We also tested the degradation of DHFR blocked with Halo at just the N-terminus (Halo-DHFR-*C*) or just the C-terminus (*N*-DHFR-Halo), where the italicized letter indicates the native DHFR terminus (Figure 7b). FtsH degraded Halo-DHFR-*C* more rapidly than *N*-DHFR-Halo. The presence of an easily identifiable major degradation product of Halo-DHFR-*C* allowed the determination of steady-state kinetic parameters for its degradation by FtsH (Figure 7c). Compared to ^{WT}DHFR, k_{deg} for the fusion protein decreased ~6-fold, whereas K_M increased ~6-fold. These changes in k_{deg} and K_M suggest that fusion of the Halo domain to the N-terminus affects FtsH binding to DHFR as well as the DHFR-unfolding step, presumed to be rate limiting for degradation. It is plausible that fusions to either terminus of DHFR hinder FtsH substrate recognition and unfolding by steric interference.

3 | DISCUSSION

We began this study by testing the hypothesis that FtsH might degrade DHFR with a degron presented on a sufficiently long, unstructured, and exposed polypeptide. At a minimum, we expected to see a DHFR product with a partially trimmed extension that would provide information about how closely degron-tagged DHFR could approach FtsH. Instead, we discovered that FtsH can degrade DHFR attached to C-terminal ssrA tails of different lengths and DHFR lacking an appended degron. We do not know why a previous study failed to observe FtsH degradation of DHFR with an appended ssrA degron.[17] Because the concentration of the radiolabeled substrate in that study was not known, it is possible that degradation could have been very slow if this concentration was far below the K_M. Differences in how FtsH or the substrates were purified might also account for the discrepancy between our results and the previous report.

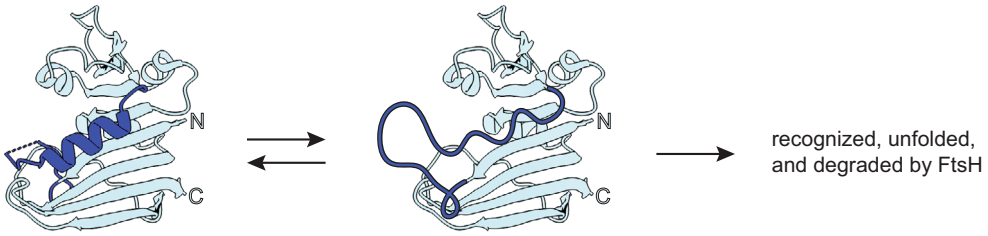

FIGURE 8 Model for FtsH recognition and degradation of DHFR. Native DHFR (left, missing density in the M20 loop shown as a dotted line) equilibrates with a species (right) in which the dark blue segment unfolds, and is then degraded by FtsH. In principle, numerous partially denatured species could exist that are recognized, unfolded, and degraded by FtsH

Although the steady-state degradation parameters are similar for ssrA-tagged and untagged DHFR variants, untagged DHFR and DHFR-ssrA[11] have slightly weaker K_M and slightly higher k_{deg} values compared to DHFR-ssrA[19] and DHFR-ssrA[40]. These small differences probably reflect the fact that degradation of the ssrA-tagged substrates can initiate at the ssrA tag or within DHFR, potentially altering binding and/or how force is applied to unfold the substrate,[37,38] and the fact that fewer amino acids need to be translocated to complete degradation of the shorter substrates.

3.1 | FtsH recognition of partially unfolded DHFR

In the simplest case, a single short unstructured peptide exposed to a native protein can act both as a recognition determinant and as the initiation site where translocation through the axial channel begins the unfolding and subsequent degradation of a substrate by a AAA+ protease. For example, appending just the C-terminal pentapeptide of the ssrA tag to the last structured residue at the C-terminus of GFP is sufficient for its degradation by ClpXP.[39] However, the only unstructured region in native DHFR is a small segment of the M20 loop,[22] which is dispensable for FtsH degradation. Thus, it is highly unlikely that FtsH recognizes native DHFR. In globally denatured DHFR, the N and C termini and other peptide sequences would be exposed and could be bound by FtsH. Importantly, however, FtsH degrades the hyper-stable A145T variant of DHFR slightly faster than the parental protein. As globally denatured ^{A145T}DHFR should be present at ~1% of the concentration of denatured wild-type DHFR under assay conditions, the fully denatured recognition model incorrectly predicts that ^{A145T}DHFR should be degraded far more slowly than ^{WT}DHFR. We conclude that FtsH is also unlikely to recognize fully denatured DHFR as its primary target.

Because biophysical studies have identified metastable intermediates in DHFR folding/unfolding,[31–33,40] we propose that one or more of these species are recognized by FtsH (Figure 8). At the temperatures (37–42°C) we used for degradation, these partially folded molecules should be populated at reasonable levels in equilibrium with native DHFR and would have unstructured regions for engagement as well as native regions that might provide additional recognition determinants.[40,41] We note that this model predicts that any DHFR mutation that increases the equilibrium population of the intermediate without directly affecting recognition would result in faster degradation by FtsH, a result that we observed for many mutant DHFR variants.

3.2 | Possibility of multiple degrons within DHFR

Mutation of residues 28 and 29, present in peptide-binding region 1, slowed FtsH degradation modestly, suggesting that these residues make up a part of a more complex recognition element. It is possible that one sequence element in partially unfolded DHFR binds FtsH, allowing a second disordered region to bind non-specifically in the axial channel to initiate engagement and translocation. There are multiple precedents for two-part-degron models in other AAA+ proteases. For example, most substrates of the 26S proteasome have a polyubiquitin moiety that binds to the 19S regulatory particle and an unstructured region that is needed to initiate proteolysis.[42,43] Similarly, some substrates of ClpXP and ClpAP have one sequence that tethers the substrate to the N-terminal domains of these proteases and another sequence that is engaged in the axial pore.[44,45]

In the absence of a long unstructured polypeptide that contains a degron, our results suggest that untagged DHFR must approach FtsH closely enough to allow recognition and engagement of a partially folded substrate, presumably by the FtsH central pore. Recent structural

insights from bacterial FtsH homologs in membranous environments indicate that it may be possible for the cytosolic portion of FtsH to engage a cytosolic substrate of considerable size without requiring a degron to be at the end of a long, flexible segment. For example, cryo-EM structures of FtsH from *Aquifex aeolicus* and *Thermotoga maritima* show that the cytoplasmic domain of FtsH can tilt with respect to the membrane, leaving a gap of ~30 Å, which could allow interaction with a partially unfolded DHFR substrate lacking a long degron tail.[46,47] We also note that our studies used detergent-solubilized FtsH and thus we do not know how being in a native membrane environment could affect the ability of FtsH to degrade DHFR.

3.3 | Implications of internal recognition

The N- or C-terminal sequences of DHFR do not bind FtsH in peptide-blot experiments, and blocking these sequences by fusion to Halo did not prevent DHFR degradation. These results suggest that FtsH recognition of untagged DHFR is noncanonical and involves engagement of internal DHFR sequences. This model, in turn, predicts that FtsH must be able to translocate multiple polypeptide strands simultaneously, an activity that has been demonstrated for the 26S proteasome, ClpXP, and HslUV.[48–52] FtsH degradation of other substrates has also been proposed to depend on the engagement of internal sequences and/or non-native conformations.[53–56] One biological consequence of internal engagement by FtsH would be an ability to degrade inner-membrane proteins whose topologies place both their N- and C-termini in the periplasm. The rate of substrate unfolding by AAA+ proteases can depend on whether the enzyme is pulling from the N- or C-terminus or an internal position, as mechanical stability can vary with the direction of the unfolding force.[23,26,37,38,57,58] In principle, therefore, recognition of internal degrons might allow FtsH to unfold proteins that would be more difficult to denature by pulling on a terminal degron.

3.4 | Is FtsH a weak protein unfoldase?

The inability of FtsH to degrade degron-tagged DHFR was originally cited as one piece of evidence for a weak unfoldase activity.[17] Although we find that FtsH does degrade DHFR, our results suggest that the actual target may be a less stable intermediate in folding/unfolding, leaving the question of unfolding strength open. The finding that FtsH can extract and degrade the stable GlpG protein from the membrane provides the strongest evidence that FtsH possesses a robust unfolding activity.[18,19] In general, however, we note that AAA+ proteases and substrates co-evolve to allow the degradation of appropriate cellular proteins when necessary. Thus, we find it unlikely that the substrate specificity of the only membrane-bound AAA+ protease in most bacteria and eukaryotic organelles is limited by an inherently weak unfoldase activity.

4 | MATERIALS AND METHODS

4.1 | Strains, plasmids, and proteins

E. coli strain T7 Express (NEB) was used for FtsH expression. For the expression of other proteins, *E. coli* strain ER2566 (NEB) was used. Constructs containing *E. coli* DHFR were expressed from HTUA vectors. *E. coli* FtsH was expressed from a pET21b vector. FtsH was purified as described.[15] For the preparation of ^{35}S-labeled FtsH for the spot-array assay, *E. coli* T7 Express cells harboring a pET21-based plasmid with a gene encoding FtsH-myc-H_6 were grown in 750 ml of minimal media (without methionine or cysteine) to log-phase and induced with 0.5 mM IPTG and EasyTag™ EXPRESS ^{35}S Protein Labeling Mix (20 μCi/ml, PerkinElmer) for 3 hr at 30°C. The harvested pellet was subjected to three cycles of freeze–thaw and then resuspended in lysis buffer (50 mM Tris–HCl, pH 8.0, 100 mM NaCl, 20 mM imidazole, 10% glycerol) before incubating with lysozyme and BugBuster reagent (Sigma Aldrich) at 4°C for 20 min. ^{35}S-FtsH was purified by Ni^{++}-NTA affinity.[15] After dialyzing into lysis buffer overnight at 4°C, the solution was flash frozen for storage at −80°C.

Cells expressing untagged DHFR, mutants of untagged DHFR, and DHFR with ssrA tails were grown in LB broth to log phase, induced with 1 mM IPTG, harvested by centrifugation, and resuspended in Q buffer (25 mM HEPES, pH 7.5, 50 mM NaCl, and 10% glycerol) for storage. After thawing, sonication, and centrifugation, the supernatant was loaded onto a Source-Q anion-exchange column and eluted using a 0–50% gradient from Q buffer to Q buffer plus 750 mM NaCl. Fractions were analyzed by SDS-PAGE, pooled, and further purified by Superdex-75 size-exclusion chromatography in DHFR storage buffer (25 mM HEPES, pH 7.5, 150 mM KCl, and 10% glycerol). Fractions containing pure protein were pooled, concentrated, and flash frozen for storage at −80°C.

The C-terminal tail (linker/degron) sequences of DHFR-ssrA[19], DHFR-ssrA[25], DHFR-ssrA[40], and DHFR-ssrA[60] were GS**H_6***AANDENYALAA*, GSHLGLTS**H_6***AANDENYALAA*,

GSHLGLIEVEKPLYGVEPFVGTS**H_6***AANDENYALAA*, and GSHLGLIEVEKPLYGVEPFVGETAHFEIELSEPDVHGQWKLTS**H_6***AANDENYALAA*, respectively (^{V13P}titin^{I27} sequences underlined; H_6 sequence; ssrA-tag sequence in italics). DHFR-ssrA^{19}, DHFR-ssrA^{25}, DHFR-ssrA^{40}, and DHFR-ssrA^{60} were purified by Ni^{++}-NTA affinity chromatography, Source-15Q anion-exchange chromatography, and Superdex-75 size-exclusion chromatography, and stored frozen.

Constructs containing Halo were initially purified fused to an N-terminal H_7-SUMO domain, purified by Ni^{++}-NTA affinity chromatography, cleaved with Ulp1 protease overnight in dialysis buffer, and passed over a second Ni^{++}-NTA affinity column to remove the cleaved H_7-SUMO protein and His-tagged Ulp1, and finally purified by Superdex-200 size-exclusion chromatography in DHFR storage buffer. Purified Halo fusion proteins were pooled, concentrated, and then labeled at molar ratios of 1 HaloTag TMR ligand (Promega) to 3 proteins for 15 min at room temperature. TMR-ligand-bound proteins were desalted using Zeba columns (Thermo Scientific) into DHFR storage buffer and flash frozen for storage at −80°C before use in degradation reactions.

4.2 | Gel assays of degradation

Substrates and enzymes were incubated at 37°C or 42°C in PD buffer (50 mM Tris–HCl, pH 8.0, 10 mM KCl, 5 mM $MgSO_4$, 10 μM $ZnCl_2$, 10% glycerol, 2 mM β-mercaptoethanol, and 0.1% Igepal CA-630) supplemented with ATP (4 mM) and a regeneration system (16 mM creatine phosphate, 75 μg/ml creatine kinase). Samples were quenched at different times by the addition of SDS-loading buffer and heated before separation by SDS-PAGE, and visualized by Coomassie staining or by TMR fluorescence. Gels were imaged using a Typhoon FLA7000 (GE Healthcare) with the Coomassie setting or Alexa 532 setting. ATP-hydrolysis rates were measured using a NADH-coupled continuous spectrophotometric assay.[59]

4.3 | Enzyme kinetics

Alexa 488-maleimide (Thermo Fisher) was used to label DHFR or its ssrA-tail variants. Different concentrations of fluorescent protein were incubated at 37°C with $FtsH_6$ (0.5 μM) in PD buffer with ATP (4 mM) and a creatine-kinase regeneration system. At different times, samples were quenched by the addition of trichloroacetic acid (final 10% v/v) and allowed to precipitate overnight at 4°C. After centrifugation, the soluble fraction was monitored for fluorescence (excitation 495 nm; emission 515 nm).

4.4 | Peptide array

Peptides of 15 amino acids were synthesized by standard Fmoc techniques using a ResPep SL peptide synthesizer (Intavis) linked via their C-termini to a cellulose membrane. Arrays were washed with TBST (TBS + 0.1% Tween20) 3×, and blocked overnight with blocking solution (TBST plus 5% bovine serum albumin) at room temperature. Blocked arrays were washed twice with TBST and then washed twice with binding buffer (50 mM Tris–HCl, pH 8.0, 100 mM KCl, 5 mM $MgSO_4$, 10 μM $ZnCl_2$, 10% glycerol, 2 mM βME, and 0.03% Igepal CA-630). The washed array was incubated with binding buffer, 0.5% BSA, 30 nM ^{35}S-FtsH, and 1.25 mM ATPγS for 1 hr at 4°C. After this incubation, the array was washed briefly with binding buffer and 1 mM ATP for 5 min at 4°C, dried, exposed to a Storage Phosphor Screen (Amersham) overnight at room temperature, and imaged using a Typhoon FLA7000 (GE Healthcare).

AUTHOR CONTRIBUTIONS

Juhee P. Morehouse: Conceptualization (equal); investigation (lead); writing – original draft (equal); writing – review and editing (equal). **Tania A. Baker:** Conceptualization (equal); funding acquisition (supporting); project administration (supporting); supervision (equal); writing – original draft (supporting); writing – review and editing (equal). **Robert T. Sauer:** Conceptualization (equal); funding acquisition (lead); project administration (lead); supervision (equal); writing – original draft (equal); writing – review and editing (equal).

ACKNOWLEDGMENTS

We thank present and former Sauer and Baker group members for helpful advice and materials, especially Tristan Bell, Sanjay Hari, Meghann Kasal, Sora Kim, and Igor Levchenko. This work was supported by NIH grant AI-16892.

CONFLICT OF INTEREST

The authors have no conflicts of interest.

DATA AVAILABILITY STATEMENT

The data that support the findings of this study are available from the corresponding author upon reasonable request.

ORCID

Robert T. Sauer https://orcid.org/0000-0002-1719-5399

REFERENCES

1. Sauer RT, Baker TA. AAA+ proteases: ATP-fueled machines of protein destruction. Annu Rev Biochem. 2011;80:587–612.
2. Varshavsky A. Naming a targeting signal. Cell. 1991;64:13–15.
3. Mahmoud SA, Chien P. Regulated proteolysis in bacteria. Annu Rev Biochem. 2018;87:677–696.
4. Davis C, Spaller BL, Matouschek A. Mechanisms of substrate recognition by the 26S proteasome. Curr Opin Struct Biol. 2021;67:161–169.
5. Olivares AO, Baker TA, Sauer RT. Mechanistic insights into bacterial AAA+ proteases and protein-remodelling machines. Nat Rev Microbiol. 2016;14:33–44.
6. Sauer RT, Bolon DN, Burton BM, et al. Sculpting the proteome with AAA+ proteases and disassembly machines. Cell. 2004; 119:9–18.
7. Ogura T, Tomoyasu T, Yuki T, et al. Structure and function of the *ftsH* gene in *Escherichia coli*. Res Microbiol. 1991;142: 142279–142282.
8. Langklotz S, Baumann U, Narberhaus F. Structure and function of the bacterial AAA protease FtsH. Biochim Biophys Acta. 2012;1823:40–48.
9. Bittner LM, Arends J, Narberhaus F. When, how and why? Regulated proteolysis by the essential FtsH protease in *Escherichia coli*. Biol Chem. 2017;398:625–635.
10. Ito K, Akiyama Y. Cellular functions, mechanism of action, and regulation of FtsH protease. Annu Rev Microbiol. 2005;59: 211–231.
11. Keiler KC, Waller PR, Sauer RT. Role of a peptide tagging system in degradation of proteins synthesized from damaged messenger RNA. Science. 1996;271:990–993.
12. Herman C, Thevenet D, Bouloc P, Walker GC, D'Ari R. Degradation of carboxy-terminal-tagged cytoplasmic proteins by the *Escherichia coli* protease HflB (FtsH). Genes Dev. 1998;12: 1348–1355.
13. Gottesman S, Roche E, Zhou YN, Sauer RT. The ClpXP and ClpAP proteases degrade proteins with carboxy-terminal peptide tails added by the SsrA-tagging system. Genes Dev. 1998; 12:1338–1347.
14. Fuhrer F, Muller A, Baumann H, Langklotz S, Kutscher B, Narberhaus F. Sequence and length recognition of the C-terminal turnover element of LpxC, a soluble substrate of the membrane-bound FtsH protease. J Mol Biol. 2007;372:485–496.
15. Hari SB, Sauer RT. The AAA+ FtsH protease degrades an ssrA-tagged model protein in the inner membrane of *Escherichia coli*. Biochemistry. 2016;55:5649–5652.
16. Kobiler O, Koby S, Teff D, Court D, Oppenheim Amos B. The phage λ CII transcriptional activator carries a C-terminal domain signaling for rapid proteolysis. Proc Natl Acad Sci U S A. 2002;99:14964–14969.
17. Herman C, Prakash S, Lu CZ, Matouschek A, Gross CA. Lack of a robust unfoldase activity confers a unique level of substrate specificity to the universal AAA protease FtsH. Mol Cell. 2003; 11:659–669.
18. Yang Y, Guo R, Gaffney K, et al. Folding-degradation relationship of a membrane protein mediated by the universally conserved ATP-dependent protease FtsH. J Am Chem Soc. 2018; 140:4656–4665.
19. Yang Y, Gunasekara M, Muhammednazaar S, Li Z, Hong H. Proteolysis mediated by the membrane-integrated ATP-dependent protease FtsH has a unique nonlinear dependence on ATP hydrolysis rates. Protein Sci. 2019;28:1262–1275.
20. Rood JI, Williams JW. Characterization of the cloned *Escherichia coli* dihydrofolate reductase. Biochim Biophys Acta. 1981; 660:214–218.
21. Touchette NA, Perry KM, Matthews CR. Folding of dihydrofolate reductase from *Escherichia coli*. Biochemistry. 1896;25: 5445–5452.
22. Bystroff C, Kraut J. Crystal structure of unliganded *Escherichia coli* dihydrofolate reductase. Ligand-induced conformational changes and cooperativity in binding. Biochemistry. 1991;30: 2227–2239.
23. Lee C, Schwartz MP, Prakash S, Iwakura M, Matouschek A. ATP-dependent proteases degrade their substrates by processively unraveling them from the degradation signal. Mol Cell. 2001;7:627–637.
24. Raimondi MV, Randazzo O, La Franca M, et al. DHFR inhibitors: reading the past for discovering novel anticancer agents. Molecules. 2019;24:1140.
25. Amberg-Johnson K, Hari SB, Ganesan SM, et al. Small molecule inhibition of apicomplexan FtsH1 disrupts plastid biogenesis in human pathogens. Elife. 2017;6:e29865.
26. Kenniston JA, Baker TA, Fernandez JM, Sauer RT. Linkage between ATP consumption and mechanical unfolding during the protein processing reactions of an AAA+ degradation machine. Cell. 2003;114:511–520.
27. Sawaya MR, Kraut J. Loop and subdomain movements in the mechanism of *Escherichia coli* dihydrofolate reductase: crystallographic evidence. Biochemistry. 1997;36: 586–603.
28. Ohmae E, Ishimura K, Iwakura M, Gekko K. Effects of point mutations at the flexible loop alanine-145 of *Escherichia coli* dihydrofolate reductase on its stability and function. J Biochem. 1998;123:839–846.
29. Ohmae E, Sasaki Y, Gekko K. Effects of five-tryptophan mutations on structure, stability and function of *Escherichia coli* dihydrofolate reductase. J Biochem. 2001;130:439–447.
30. Arai M, Maki K, Takahashi H, Iwakura M. Testing the relationship between foldability and the early folding events of dihydrofolate reductase from *Escherichia coli*. J Mol Biol. 2003;328: 273–288.
31. Kuwajima K, Garvey EP, Finn BE, Matthews CR, Sugai S. Transient intermediates in the folding of dihydrofolate reductase as detected by far-ultraviolet circular dichroism spectroscopy. Biochemistry. 1991;30:7693–7703.
32. Heidary DK, O'Neill JC Jr, Roy M, Jennings PA. An essential intermediate in the folding of dihydrofolate reductase. Proc Natl Acad Sci U S A. 2000;97:5866–5870.
33. Kasper JR, Liu P-F, Park C. Structure of a partially unfolded form of *Escherichia coli* dihydrofolate reductase provides insight into its folding pathway. Protein Sci. 2014;23:1728–1737.
34. Yamamoto T, Izumi S, Gekko K. Mass spectrometry on segment-specific hydrogen exchange of dihydrofolate reductase. J Biochem. 2004;135:17–24.
35. Zuromski KL, Sauer RT, Baker TA. Modular and coordinated activity of AAA+ active sites in the double-ring ClpA unfoldase of the ClpAP protease. Proc Natl Acad Sci U S A. 2020;117: 25455–25463.

36. Los GV, Encell LP, McDougall MG, et al. HaloTag: a novel protein labeling technology for cell imaging and protein analysis. ACS Chem Biol. 2008;3:373–382.
37. Olivares AO, Kotamarthi HC, Stein BJ, Sauer RT, Baker TA. Effect of directional pulling on mechanical protein degradation by ATP-dependent proteolytic machines. Proc Natl Acad Sci U S A. 2017;114:E6306–E6313.
38. Kotamarthi HC, Sauer RT, Baker TA. The non-dominant AAA+ ring in the ClpAP protease functions as an anti-stalling motor to accelerate protein unfolding and translocation. Cell Rep. 2020;30:2644–2654.
39. Fei X, Bell TA, Barkow SR, Baker TA, Sauer RT. Structural basis of ClpXP recognition and unfolding of ssrA-tagged substrates. Elife. 2020;9:e61496.
40. Ionescu RM, Smith VF, O'Neill JC Jr, Matthews CR. Multistate equilibrium unfolding of *Escherichia coli* dihydrofolate reductase: Thermodynamic and spectroscopic description of the native, intermediate, and unfolded ensembles. Biochemistry. 2000;39:9540–9550.
41. Ohmae E, Kurumiya T, Makino S, Gekko K. Acid and thermal unfolding of *Escherichia coli* dihydrofolate reductase. J Biochem. 1996;120:946–953.
42. Prakash S, Tian L, Ratliff KS, Lehotzky RE, Matouschek A. An unstructured initiation site is required for efficient proteasome-mediated degradation. Nat Struct Mol Biol. 2004;11:830–837.
43. Inobe T, Fishbain S, Prakash S, Matouschek A. Defining the geometry of the two-component proteasome degron. Nat Chem Biol. 2011;7:161–167.
44. Neher SB, Sauer RT, Baker TA. Distinct peptide signals in the UmuD and UmuD′ subunits of UmuD/D′ mediate tethering and substrate processing by the ClpXP protease. Proc Natl Acad Sci U S A. 2003;100:13219–13224.
45. Hoskins JR, Wickner S. Two peptide sequences can function cooperatively to facilitate binding and unfolding by ClpA and degradation by ClpAP. Proc Natl Acad Sci U S A. 2006;103:909–914.
46. Carvalho V, Prabudiansyah I, Kovacik L, et al. The cytoplasmic domain of the AAA+ protease FtsH is tilted with respect to the membrane to facilitate substrate entry. J Biol Chem. 2021;296:100029.
47. Liu W, Schoonen M, Wang T, McSweeney S, Liu Q. Cryo-EM structure of transmembrane AAA+ protease FtsH in the ADP state. Commun Biol. 2022;5:257.
48. Burton RE, Siddiqui SM, Kim YI, Baker TA, Sauer RT. Effects of protein stability and structure on substrate processing by the ClpXP unfolding and degradation machine. EMBO J. 2001;20:3092–1300.
49. Bolon DN, Grant RA, Baker TA, Sauer RT. Nucleotide-dependent substrate handoff from the SspB adaptor to the AAA+ ClpXP protease. Mol Cell. 2004;16:343–350.
50. Kwon AR, Trame CB, McKay DB. Kinetics of protein substrate degradation by HslUV. J Struct Biol. 2004;146:141–147.
51. Lee C, Prakash S, Matouschek A. Concurrent translocation of multiple polypeptide chains through the proteasomal degradation channel. J Biol Chem. 2002;277:34760–34765.
52. Liu CW, Corboy MJ, DeMartino GN, Thomas PJ. Endoproteolytic activity of the proteasome. Science. 2003;299:408–411.
53. Obrist M, Narberhaus F. Identification of a turnover element in region 2.1 of *Escherichia coli* sigma32 by a bacterial one-hybrid approach. J Bacteriol. 2005;187:3807–3813.
54. Obrist M, Milek S, Klauck E, Hengge R, Narberhaus F. Region 2.1 of the *Escherichia coli* heat-shock sigma factor RpoH (sigma32) is necessary but not sufficient for degradation by the FtsH protease. Microbiology (Reading). 2007;153:2560–2571.
55. Okuno T, Yamanaka K, Ogura T. An AAA protease FtsH can initiate proteolysis from internal sites of a model substrate, apo-flavodoxin. Genes Cells. 2006;11:261–268.
56. Okuno T, Yamanaka K, Ogura T. Flavodoxin, a new fluorescent substrate for monitoring proteolytic activity of FtsH lacking a robust unfolding activity. J Struct Biol. 2006;156:115–119.
57. Kenniston JA, Burton RE, Siddiqui SM, Baker TA, Sauer RT. Effects of local protein stability and the geometric position of the substrate degradation tag on the efficiency of ClpXP denaturation and degradation. J Struct Biol. 2004;146:130–140.
58. Gur E, Vishkautzan M, Sauer RT. Protein unfolding and degradation by the AAA+ Lon protease. Protein Sci. 2012;21:268–278.
59. Burton RE, Baker TA, Sauer RT. Energy-dependent degradation: linkage between ClpX-catalyzed nucleotide hydrolysis and protein-substrate processing. Protein Sci. 2003;12:893–902.

How to cite this article: Morehouse JP, Baker TA, Sauer RT. FtsH degrades dihydrofolate reductase by recognizing a partially folded species. Protein Science. 2022;31(9):e4410. https://doi.org/10.1002/pro.4410